Through alizarin-hectorite pigments: Influence of organofunctionalization on fading

Fabrícia de Castro Silva, Luciano Clécio Brandão Lima, Edson Cavalcanti Silva-Filho, Maria Gardennia Fonseca, Maguy Jaber

Through Alizarin-Hectorite pigments: influence of the organofunctionalization on dye fading

Fabrícia de Castro Silva[1,2,3], Luciano Clécio Brandão Lima[1,2], Edson Cavalcanti Silva-Filho[1], Maria Gardênnia Fonseca[4], Maguy Jaber[2*]

[1]LIMAV, Univ. Federal do Piauí – UFPI, 64049-550 Piauí, Brazil

[2]Sorbonne Université, CNRS UMR 8220, LAMS, Institut Universitaire de France (IUF), Boite courrier 225, 4 pl. Jussieu 75252 Paris cedex 05, France

[3]Campus Senador Helvídio Nunes Barros-CSHNB, Univ. Federal do Piauí – UFPI, 64607-607, PI, Brazil

[4]NPE-LACOM, Univ. Federal da Paraíba – UFPB, João Pessoa, 58051-900 Paraíba, Brazil

*Corresponding Author:

Maguy Jaber

Tel: +33-(0)1-4427-6289

Email: maguy.jaber@sorbonne-universite.fr

ABSTRACT

In this work, hectorite/alizarin pigments were prepared at pH 9 and 12. Hectorite was initially modified with cetyltrimethylammonium and pectine to produce organo-hectorites. The influence of organo-hectorite on the stabilization of alizarin was evaluated. X-ray diffraction suggested the formation of exfoliated/delaminated structures after organofunctionalization of the hectorite. For raw hectorite and their derivatives with pectin, the formation of hybrid pigments was confirmed by infrared spectroscopy. Thermogravimetry curves confirm the hectorite organofunctionalization and that the alizarin loading was higher at pH 12. The hybrids prepared at pH 12 show more photostability than ones prepared at pH 9. This behavior was probably due to the total deprotonation of dye molecules, which promoted better interactions between the hosts and the guests.
Keywords: hectorite, organofunctionalization, pigments, alizarin.

1. Introduction

Art is a form of universal language that connects culture, time and people in its various forms. Painting was the form of art chosen/developed by primitive men as a testimony of daily life, and since of then mankind has used this expression to reflect important artistic and historical values that may provide clues to the understanding of ancient culture [1–3].

Over the centuries, organic dyes have been extensively applied as a source of colors. Coming from natural sources such as animals and plants, as well as from synthetic sources after emergence of modern industrial chemistry in the 19th century, it is known that the organic dye exists in a wide range of types which can be classified by their structure, colors and/or form of attachment. Anthraquinone is a class of naturally occurring polyphenolic dyes which have been commonly used in works of art. The most important representative dye of the class is alizarin (1,2- dihydroxyanthraquinone, abbreviated as ALZ) being one of principal component occurring in Rubia tinctorum L. Alizarin was identified in textile clothes and accessories form Bronze Age and in Coptic textiles from the Romanic era (Sixth century AD) and in paintings showing its representative employ through the ages.[4–7].

Unfortunately, organic dyes suffer from poor thermostability and photostability. The techniques of painting have been improved over the years, adding value to this form of artwork, and the enhancement of the dye stability has been a great challenge that interest for artists, archeologists and scientists. One possibility is to prepare organic-inorganic hybrid pigments where a strong interaction between organic chromophores and inorganic matrices aims to obtain stable pigments [8–10].

In this perspective, with scientific advances especially in materials engineering, the development of hybrid pigments has aroused interest in the scientific community [11–17]. The clays, in particular, have been extensively exploited in this scientific field, due to their natural abundance, low acquisition cost and diversified potential of use, which is due to the ease with which these materials are chemically modified [18–21]. The inorganic cations on the clay surface (Na^+, K^+, and Ca^{2+}) can be replaced by organic cations through ion exchange and the clay surface became organophilic [22].

The use of clays for the preparation of organic-inorganic hybrid pigments, in order to improve stability, has been increasingly reported in the literature [23–25]. In particular, the smectite clays, which constitute a family of layered oxides with 2:1 layer lattice structures [26]. Aluminum, iron, magnesium and sometimes lithium occupy the octahedral sites, whereas silicon and, in part aluminum occupy tetrahedral sites. Various cations, but specially Na^{+} and Ca^{2+}, may occupy interlayer positions [27,28].

Hectorite ($Na_{0.3}[Si_4Mg_{2.7}Li_{0.3}]O_{10}(OH)_2$) is a smectite-like synthetic clay that is composed of stacked layered, about 0.96 nm thick [29], widely used in dye adsorption processes [30–33]. In addition its modification can improve enhancement of its characteristics in different application fields [29,34].

The quaternary ammonium salt surfactants, such as Cetyltrimethylammonium Bromide (CTABr), for clay modification are widely used. In general, these compounds incorporate long aliphatic chains and quaternary ammonium into the clays groups, improving their existing properties [35–37].

Moreover, pectin has been reported because of its ability to form gels, non-toxic nature and its low cost [38]. It is an α-galacturonic acid heteropolysaccharide with a variable number of natural water-soluble methyl ester groups extracted from the cell walls of plants [39,40].

In this work, synthetic hectorite was used as an inorganic support for the development of hybrid pigments, by means of the chemical modification of its structure with the organic agents CTA and PEC, for later reaction with alizarin dye.

2. Experimental part

2.1. Chemicals

Hydrofluoric acid (40%, wt), sodium acetate (99%, wt), magnesium acetate (99%, wt), lithium acetate (99%, wt), silica (aerosol 130), cetyltrimethylammonium bromide (99%, wt), silver nitrate (99%, wt), sodium hydroxide (98 %, wt), pectin (85% esterified), alizarin (97%, wt) and deionized water. All chemicals applied in this work were purchased from Sigma-Aldrich with an analytical grade and used without any previous purification.

2.2. Synthesis of the hectorite (Hec)

For the synthesis of sodium hectorite the reagents were mixed in the following order according to the following theoretical formula: $Na_{0.3}[Si_4Mg_{2.7}Li_{0.3}]O_{10}(OH)_2$: deionized water, hydrofluoric acid sodium acetate magnesium acetate tetrahydrate, lithium acetate and silica. The hydrogels were aged under stirring at room temperature for 2 h and then were autoclaved for reaction at 250 °C for 72 h. The autoclave was cooled to room temperature and the product was washed thoroughly with distilled water and centrifuged. The solids were then dried at 50°C for 24 h.

2.3. Synthesis of Organo-Hectorite

2.3.1. Cetyltrimethylammonium bromide hectorite (CTA_Hec)

The synthesis of modified hectorite was conducted according to a previous procedure [41]. 2.0 g of hectorite were dispersed in 100 mL of surfactant solution (0.1 mol L^{-1}) and kept under stirring at 50 °C. Three successive batches were conducted, in which the first and second batch were kept under stirring for 4 h, and the last one was kept for 16 h. After the end of each step, the solid was recovered by centrifugation and redispersed in 100 mL of 0.1 mol L^{-1} surfactant solution to perform a total cationic exchange. After the last step, the solid was separated by centrifugation and washed several times with distilled water at 50 °C until no bromide ion could be detected by an

aqueous $AgNO_3$ solution, and then dried in an oven at 50 °C for 24 h. The obtained material is noted CTA_Hec.

2.3.2. Pectin hectorite (PEC_Hec)

For pectine/hectorite hybrid, 2.0 g of Hec was dispersed in 100 mL of pectin solution (4.0 mg L^{-1}) was stirred for 16 h, then the material was centrifuged, washed and dried in an oven at 50 °C for 24 h. The obtained material is noted PEC_Hec.

2.4. Synthesis of the hybrid pigments

Hectorite and organo-modified Hectorite were loaded with alizarin (ALZ) considering the different values of pKa, that are (6.6–7.5 and 12.4–13.5) [26,42]. For each sample, 1.0 g of the Hec or Organo-Hec was added to 100 mL of alizarin (0.2 g L^{-1}) solution, the pH was adjusted to 9 or 12 with 0.1 mol L^{-1} NaOH and was left under stirring for 4 h. The samples were then centrifuged and dried at 50 °C for 24 h.

2.5. Characterization

X-ray diffraction patterns were recorded on a D8 Advance Bruker-AXS Powder X-ray diffractometer with CuKα radiation (λ = 0.15405 nm). XRD patterns were performed between 5-70° (2θ) with a scan rate of 0.05 deg. min^{-1} for samples in powder and 1-10° (2θ) with a scan rate of 0.05 deg. min^{-1} for samples prepared by clay deposit on glass slide method, where dispersions of 60 mg of clays in 1 mL of water were dropwised on a glass slide and dried at 50 °C.

Infrared spectra were carried out on an Agilent Cary 630 FTIR spectrometer using an Agilent transmission module with spectral resolution of 2 cm^{-1} and 32 scans. The solid samples were prepared by pressed KBr pellet method and spectra were acquired by Microlab FTIR Software (Agilent Technologies) between 4000 and 650 cm^{-1}.

Thermogravimetric analyses were carried out using a TA Instrument SDT Q600 analyzer. The heating rate was of 5°C min^{-1} from 25 to 1000°C, under dry air flow of 10 mL min^{-1}, and using alumina crucible.

2.6. Light-induced ageing

Ageing effects were simulated by exposure of solid pigments to white light irradiation for 192 h, using a LED lamp set to provide 100 Klx of illumination intensity, where this time is equivalent to approximately 30 years of exposure in a museum.

Spectrophotocolorimetry was performed using an Ocean OpticsHalogen and Deuterium Light Source HL-2000-FHSA device as incident light beam and ocean optics USB4000 detector for acquisition. Ocean Optics QP400-1-UV-VIS fiberglass was used to link these devices. For each acquisition, an average of 100 scans were useful to obtain the optimum signal. The reflectance wavelength range was set from 400 to 950 nm and measurements are done on pressed pellets samples as function of L*, a* and b* coordinates. The differences of colors between unexposed and exposed samples were calculated by $\sqrt{((\Delta L^*)^2 + (\Delta a^*)^2 + (\Delta b^*)^2)}$ equation, according to the “Commission Internationale of l’Eclairage” (CIE).

3. Results and Discussion

3.1. Characterization

3.1.1. X-Ray Diffraction

The results obtained by X-ray diffraction for all materials are shown in Fig. 1(I)-(III). The XRD patterns for synthesized Hec showed the characteristic reflections of hectorite at 2θ of 6.58° (d=13.44 Å), 19.63° (d=4.59 Å), 27.56° (d=3.33 Å), 35.18° (d=2.67 Å), 53.37° (d=1.92 Å) and 61.07° (d=1.76 Å) and they were assigned to [001], [110, 020], [004], [130, 200], [201] and [060, 330] typical planes of hectorite clay respectively, as reported previously [30,43].

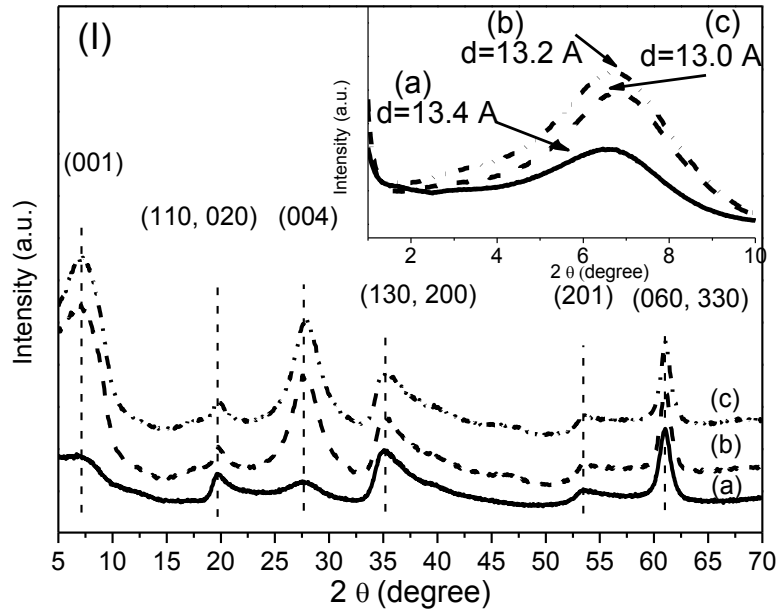

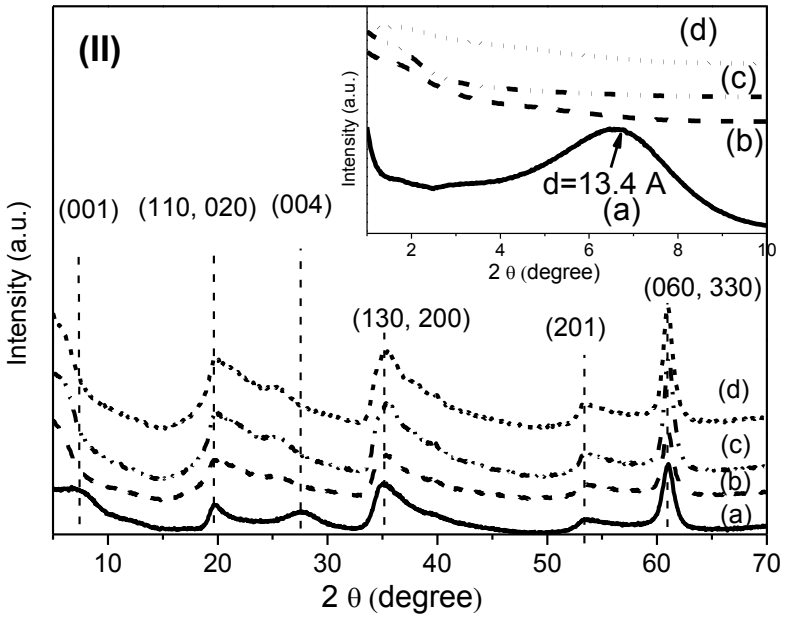

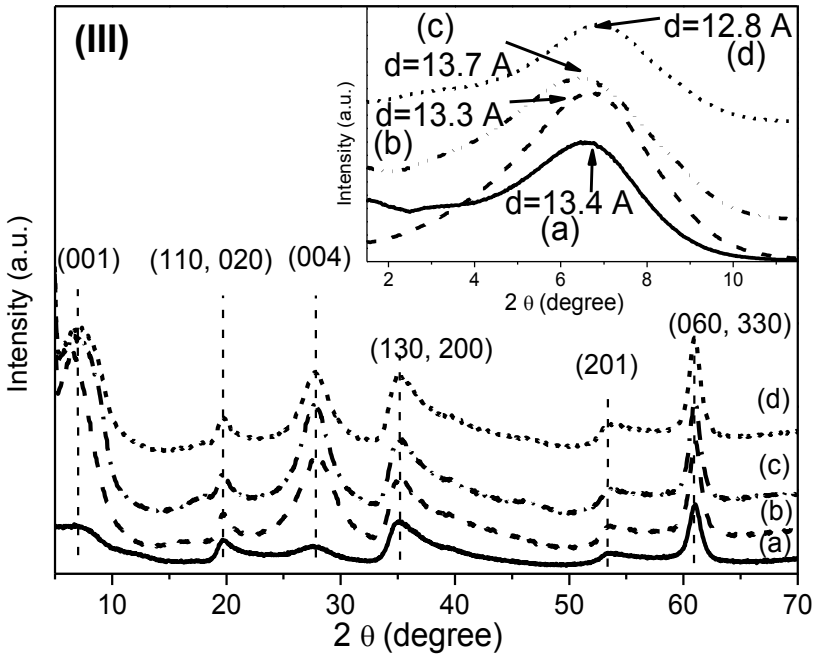

Fig. 1. XRD patterns of the precursors and hybrid pigments after loading with alizarin (I) (a) Hec, (b) Hec-ALZ at pH 9 and (c) Hec-ALZ at pH 12; (II) (a) Hec, (b) CTA_Hec, (c) CTA_Hec-ALZ at pH 9 and (d) CTA_Hec-ALZ at pH 12 and (III) (a) Hec, (b) PEC_Hec, (c) PEC_Hec-ALZ at pH 9 and (d) PEC_Hec-ALZ at pH 12, showing in insert the shift in the d_{001} peak.

Fig. 1(I) showed the X-ray diffraction patterns of the hybrid pigments obtained after ALZ loading on Hec. The direct adsorption of ALZ on Hec does not induce significant changes in the d_{001} to justify an intercalation of the dye in the interlayer space. This is probably due to the electrostatic repulsion between the surface and the deprotonated dye molecule due the pH of the medium. However, it can be noted a best definition of some reflections (i.e. [001] and [004]) that indicates a structural re-organization probably due to the intermolecular interactions between π-conjugated rings of anthraquinone dye and hydroxyl groups on the Hec edges [27].

The hybrid pigments formed after dye loading in CTA_Hec (see in Fig. 1(II)) showed a different mechanism of interaction that provide different changes in the main reflections compared to the pristine clay. In this case, the [001] reflection disappeared after exchange with the cationic surfactant, indicating probably the exfoliation/delamination of Hec layers or the presence of a heterogeneity in the layers stacking. [41,43]. After the loading with ALZ, no

significant changes were found in the composites based on CTA_Hec. Similar behavior is observed for hybrid pigments obtained after ALZ loading on PEC_Hec in X-ray patterns depicted in Fig. 1(III). The schematic representation for the possible interaction in the hybrid pigments formation are depicted in Fig. 2.

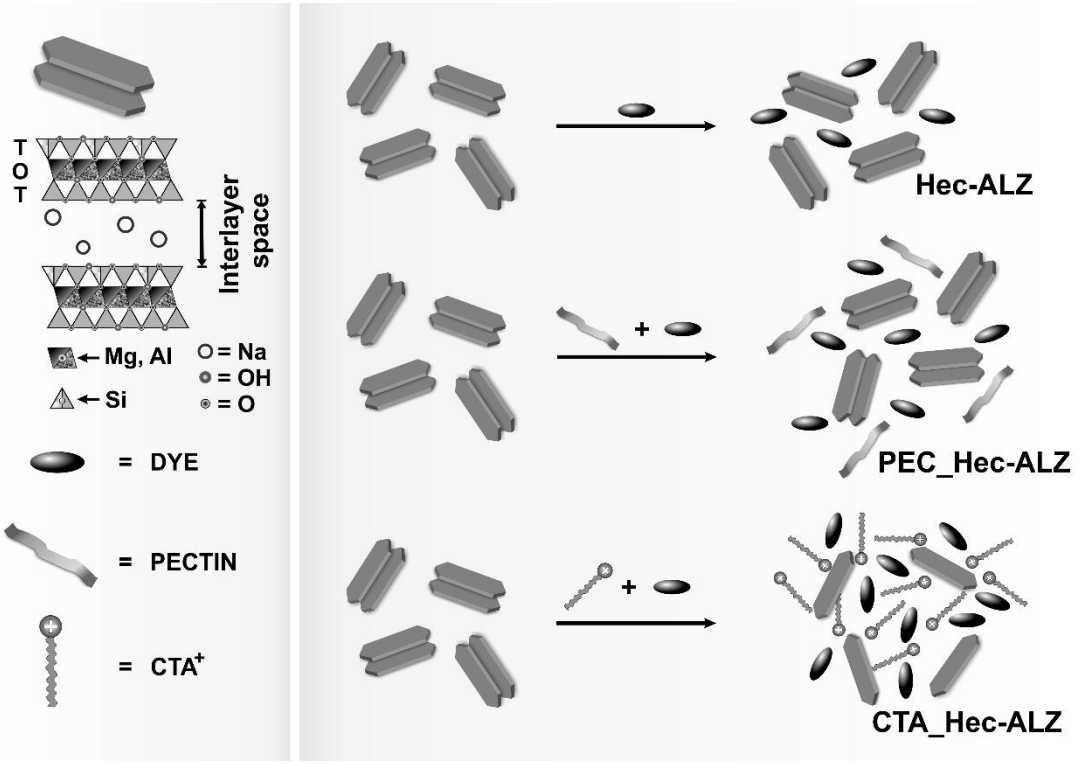

Fig. 2. Schematic representation for hybrid pigments formation.

3.1.2. FTIR

FTIR spectra of pristine hectorite and their hybrids formed are shown in Fig. 3(I)-(III).

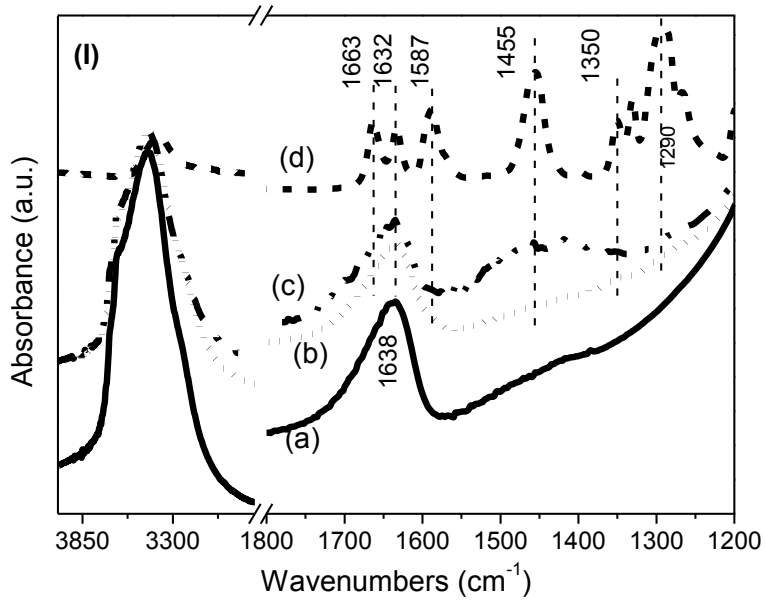
(I)
1663
1632
1587
1455
1350
1290
(d)
(c)
(b)
1638
(a)
Absorbance (a.u.)
3850
3300
1800
1700
1600
1500
1400
1300
1200
Wavenumbers (cm-1)

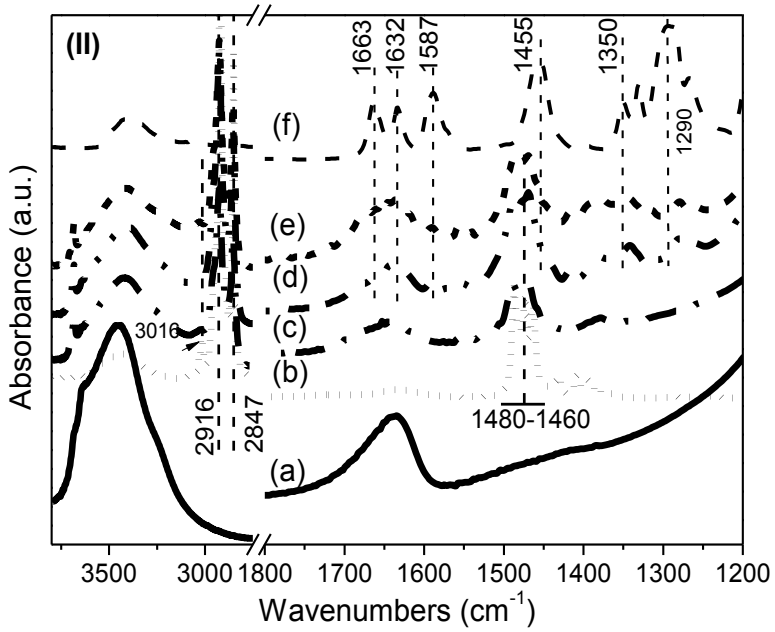
(II)
1663
1632
1587
1455
1350
1290
(f)
(e)
(d)
(c)
(b)
(a)
3016
2916
2847
1480-1460
Absorbance (a.u.)
3500
3000
1800
1700
1600
1500
1400
1300
1200
Wavenumbers (cm-1)

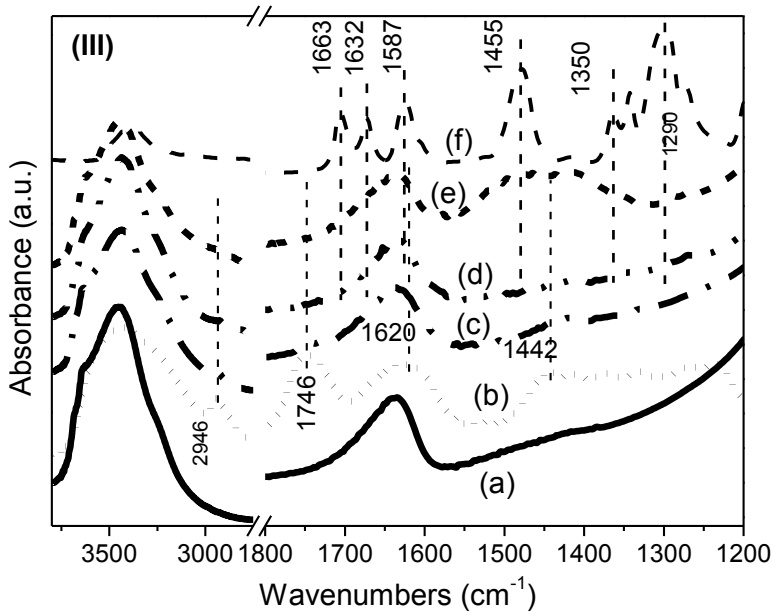

Fig. 3. ATR-IR spectra of the percursors and hybrid pigments obtained after alizarin loading (I): (a) Hec, (b) Hec-ALZ at pH 9, (c) Hec-ALZ pH 12 and (d) ALZ; (II) (a) Hec, (b) CTABr, (c) CTA_Hec, (d) CTA_Hec-ALZ at pH 9, (e) CTA_Hec-ALZ at pH 12 and (f) ALZ and (III) (a) Hec, (b) Pec, (c) Pec_Hec, (d) PEC_Hec-ALZ at pH 9, (e) PEC_Hec-ALZ at pH 12 and (f) ALZ.

Characteristic bands of hectorite can be found at about 3750-3150 cm^{-1}, assigned to the stretching vibration of structural O-H (MgO-H and SiO-H) and adsorbed water. The band at 1635 cm^{-1} is attributed to bending modes of –OH in adsorbed water molecule directly coordinated to the exchangeable cations of the clay mineral and the one at 1020 cm^{-1} is associated to the Si-O-Si stretching vibration [44,45].

The characteristic bands of CTABr are depicted in Fig. 3(II), where the $\nu_{as}[N(CH_3)_3]$ vibration is found at 3016 cm^{-1}, the absorption bands at 2916 cm^{-1} and 2847 cm^{-1} are attributed to the ν_{as}(C—H) and ν_{s}(C—H) respectively, while the region between 1460-1488 cm^{-1} correspond to the bending mode of $[N(CH_3)_3]$ and (CH_2) groups [41,46]. These characteristic peaks were observed in spectra of CTA_Hec (Fig. 3(II)) confirming the presence of CTAB in organo-Hec.

The typical absorption bands of polysaccharides are present in spectra of PEC in Fig. 3(III). The region between 3600-3000 cm^{-1} correspond to O-H stretching vibration and the band at 2946 cm^{-1} is assigned to C-H stretching

vibration. The absorption band at 1746 cm^{-1} can be assigned to C=O stretching vibration of ester carbonyl, and the non-methylated carboxyl groups are represented by absorption band at around 1620 cm^{-1}. The signal at 1442 cm^{-1} correspond to the stretching vibration of C-O bonds within COOH [47,48]. The presence of these characteristic bands in spectra of PEC_Hec (Fig. 3(III)) appears as shoulders at 2946 cm^{-1} and 1446 cm^{-1}.

The spectrum corresponding to ALZ dye showed characteristic bands related to anthraquinone groups: the (C=O) stretching of the quinone group, (C=C) aromatic stretching and OH bending appear at 1663 , 1587 and 1455 cm^{-1}, respectively [26,49].

For the Hec-ALZ hybrid pigments, the band at 1638 cm^{-1} was broader due to the contributions of ALZ bands at 1663-1587 cm^{-1} ((C = O) and υ (C = C)) adsorbed on the clay surface. The same observation for the hybrid pigment prepared at pH 12, the band at 1455 cm^{-1} assigned to δ (OH) is broad. The hybrid pigments based on CTA_Hec presented ALZ bands with some alterations, and bands at 1663 cm^{-1} and 1632 cm^{-1} appeared as a single broad band. The catechol functions observed at 1290 cm^{-1} are shifted to 1285, possibly due to the interaction between -OH of the dye and the ones on the edges of Hec. For PEC_Hec-ALZ, slight changes mainly for hybrid obtained at pH 12, in which a wide band between 1559 and 1330 cm^{-1} occurred and is associated to vibrations of the groups of both ALZ and PEC.

3.1.3. Thermal analysis (TG/DTG)

Thermogravimetry was used for monitoring of the thermal stability of the solids. DTG curves for all samples are shown in Fig. 4. For Hec sample, the first mass loss was observed at temperatures below 100 °C, more precisely at T_{max} = 56 °C, with a mass loss about 8.1%, attributed to the departure of physisorbed water [30, 45].

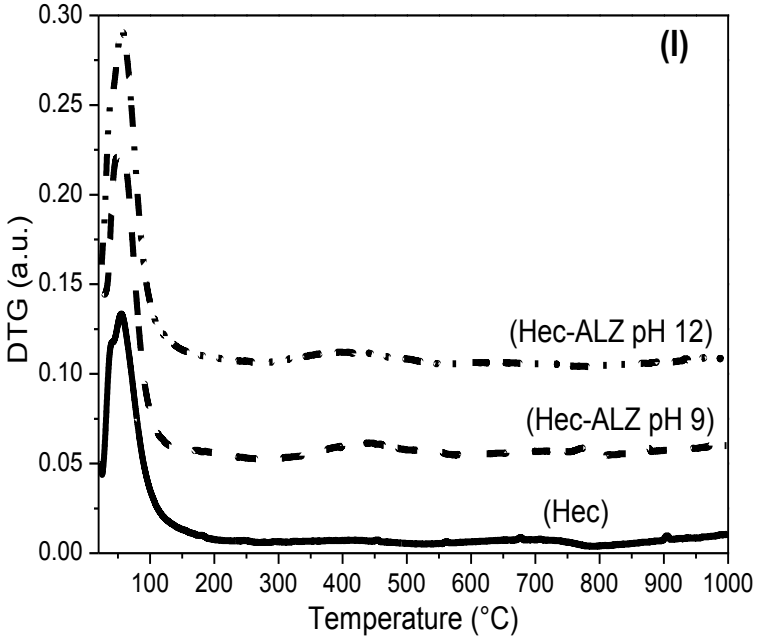
(I)
DTG (a.u.)
Temperature (°C)
(Hec-ALZ pH 12)
(Hec-ALZ pH 9)
(Hec)

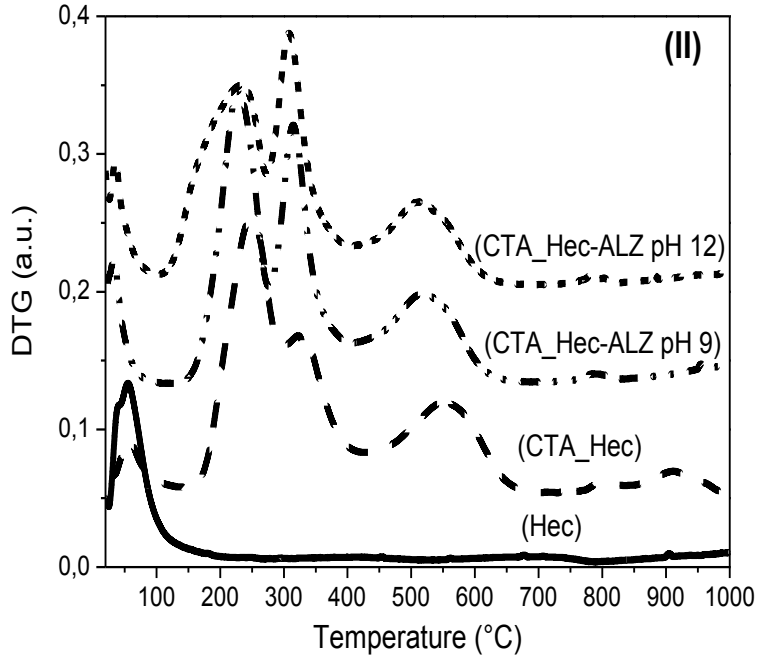
(II)
DTG (a.u.)
Temperature (°C)
(CTA_Hec-ALZ pH 12)
(CTA_Hec-ALZ pH 9)
(CTA_Hec)
(Hec)

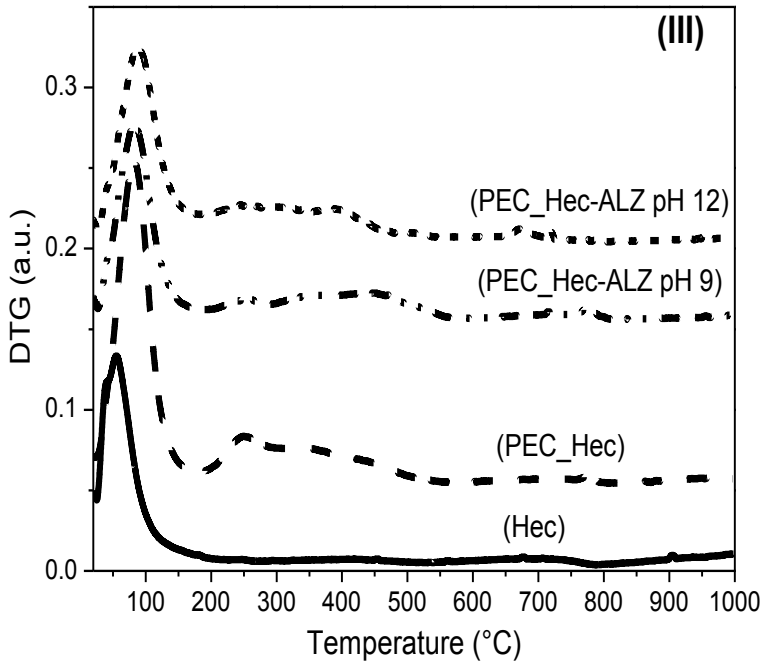

Fig. 4. DTG curves of the precursors and hybrid pigments based on (I) Hec; (II) CTA_Hec and (III) PEC_Hec.

The DTG curves of the hybrid pigments showed a second event in broader temperature range (108 and 662 °C) with different shapes depending on the composition and the amount of organic matter. For the hybrid pigment obtained with ALZ and Hec, the second event occurred between 270-590 °C with T_{max} = 434 °C and 405 °C for Hec-ALZ at pH 9 and Hec-ALZ at pH 12 respectively, which corresponds to the mass loss of 2.25% and 2.85% of alizarin dye respectively (Fig. 4(I)).

The DTG curve of sample prepared with PEC (Fig. 4(III)) presents a change in the first event of mass loss from T_{max} = 56 °C to T_{max} = 83 °C for Hec and PEC_Hec respectively, probably due the new intermolecular interaction formed with pectin molecules that promote more strong interaction with physisorbed water and also increase of its amount (mass loss increased from 8.14% to 13.02% in Hec and PEC_Hec respectively). After ALZ loading, the first event was not changed. However, a decrease in the mass loss from 13.02% to 8.92% and 9.42% for PEC_Hec, PEC_Hec-ALZ at pH 9 and PEC_Hec-ALZ at pH 12 respectively, was observed. The second event occurred between 170-560 °C with mass losses of 7.44%, 7.03% and 7.35% for PEC_Hec, PEC_Hec-

ALZ at pH 9 and PEC_Hec-ALZ at pH 12, respectively. All TG results are summarized in Table 1.

Table 1 Temperatures and percentages of mass loss in each event calculated by thermal analysis.

Samples	Event	Temperature Range (°C)	Mass Loss (%)
Hec	1	20-165	8.2
	2	–	–
Hec-ALZ pH 9	1	25-270	9.5
	2	270-590	2.3
Hec-ALZ pH 12	1	25-170	11.4
	2	243-560	2.8
PEC_Hec	1	22-170	13
	2	170-560	7.4
PEC_Hec-ALZ 9	1	25-192	8.9
	2	192-634	7
PEC_Hec-ALZ 12	1	20-180	9.4
	2	180-555	7.4
CTA_Hec	1	25-105	2.2
	2	105-690	37
CTA_Hec-ALZ 9	1	25-117	2.6
	2	117-670	37.4

CTA_Hec-ALZ 12	1	20-104	3.5
	2	104-670	38.2

As shown in Fig. 4(II) and Table 1, the DTG curves for hybrid pigments based on CTA_Hec exhibit a reduction in the mass loss below 100°C attributed to the adsorbed water, from 8.14% to 2.19% for Hec and CTA_Hec respectively, indicating an enhancement of surface hydrophobicity, as can be seen in Fig. 5 [50]. After dye loading, the T_{max} for water loss change for lower temperatures at about 35 °C, confirming the weak interaction of the surface and the physisorbed water. In this case, the second event associated to organic degradation occurs between 105-690 °C associated with three mass losses of 37.00%, 37.40% and 38.15% for CTA_Hec, CTA_Hec-ALZ pH 9 and CTA_Hec-ALZ pH 12 respectively and confirm the greater amount of organic matter incorporated than in the other hybrids.

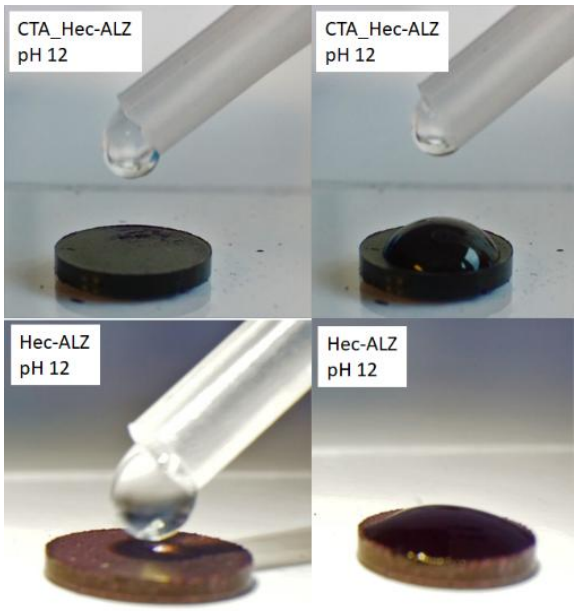

Fig. 5. Qualitative hydrophobicity test for CTA_Hec-ALZ pH12 and Hec-ALZ pH12.

3.2. Light-induced ageing

Alizarin has two different values of pK_a (6.6–7.5 and 12.4–13.5). ALZ solution is yellow and neutral (charge 0) at pH below 5.2 (Fig. 6). At pH 6–10, it

is deprotonated (charge -1, monovalent anions) and red. Finally, a violet di-anionic form (charge -2) is present at pH close 12 [26].

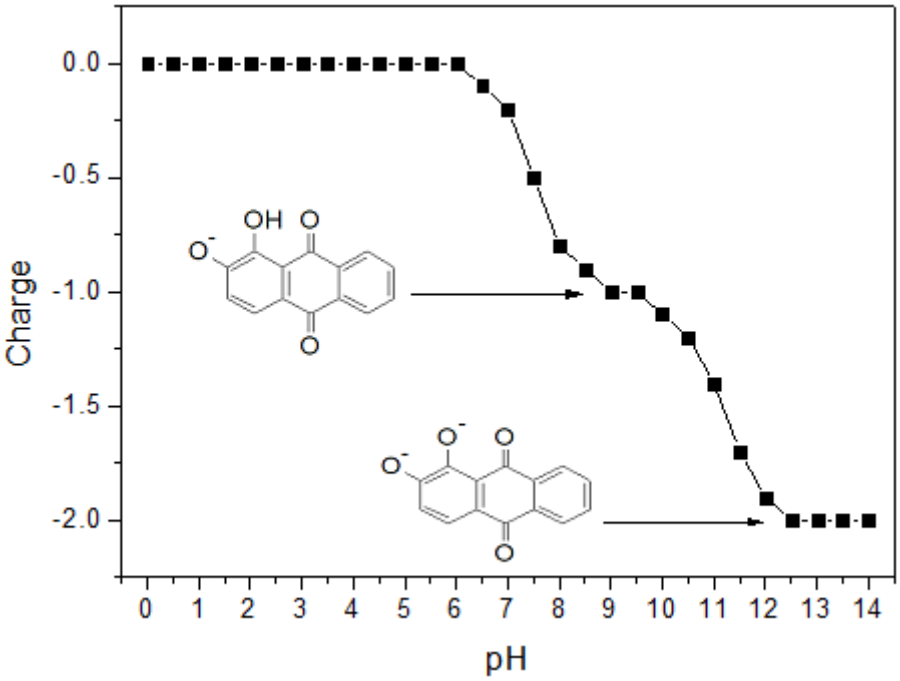

Fig. 6. Speciation diagram of Alizarin (calculated from the microspecies plugin of the calculator plugin in MarvinSketch 19.11).

The speciation of alizarin in the hybrid pigments (prepared at pH 9 or 12) enables different possible interactions with the mineral. The Hec and PEC_Hec have negative residual charges due the dissociation of the polysaccharide (for PEC_Hec) and the clay surface. As the dye molecules are negatively charged at this pH (charge -1 at pH 9 and -2 at pH 12), electrostatic repulsion can occur between the dye and the hosts. Therefore, the interactions can be driven by weak attractions like van der walls forces and/or hydrogen bonds. The similarity in respective colors of solid pigments, as can be seen in Fig. 7(I)-(III), also support the hypotheses of similar interactions for HEC-ALZ and PEC_HEC-ALZ samples. On the other hand, the pigments based on CTA_Hec showed different colors in comparison to those based on Hec and PEC_Hec (Fig. 7(I)). This behavior indicates different interactions o-clay/dye, it is probably due to the possible electrostatic attraction between the intercalated CTA^+ and ALZ negatively charged species.

The different intermolecular interactions also influence the behavior of the dye released in water, as can be seen in Fig. 7(II). The higher forces of

attractions in the pigments based on CTA_Hec explain the retention of the dye, while the weakly intermolecular interaction for the hybrids based on Hec and PEC_Hec allowed a slight release of the dye in water.

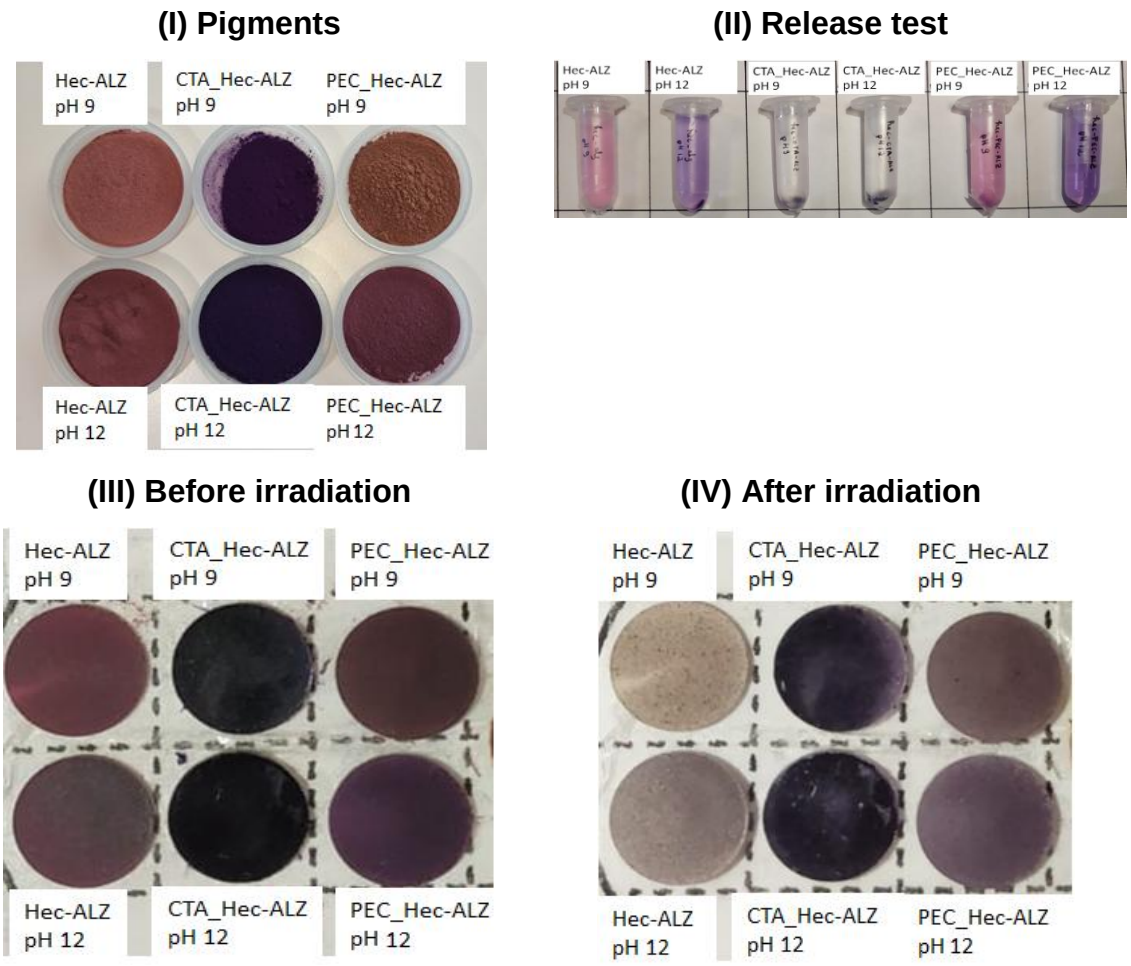

Fig. 7. Images of (I) Pigments obtained at different pH, (II) Release tests in water (III) Pigments before and (IV) after LED irradiation.

Studies have shown the irreversible damages caused to pigments by a long time of light exposure [51]. The hybrid pigments were pressed into pellets and placed under light exposure during 192 h (this time is equivalent to approximately 30 years of exposure in a museum) (Fig. 6(III)-(IV)).

To better understand the color change, the reflectance spectra of samples before and after exposure (see in Fig. 8), as well as the evolution of color differences during exposition time (see in Fig. 9) were recorded to evaluate the color stability of hybrid pigments.

It can be noticed that the reflectance spectra for pigments based on Hec showed a shift at higher values of reflectance. It is probably due to the fading of the dye as observed in Fig. 7. In general, the other hybrids present similar

spectra after irradiation, suggesting less variation of colors and consequently higher resistance [26].

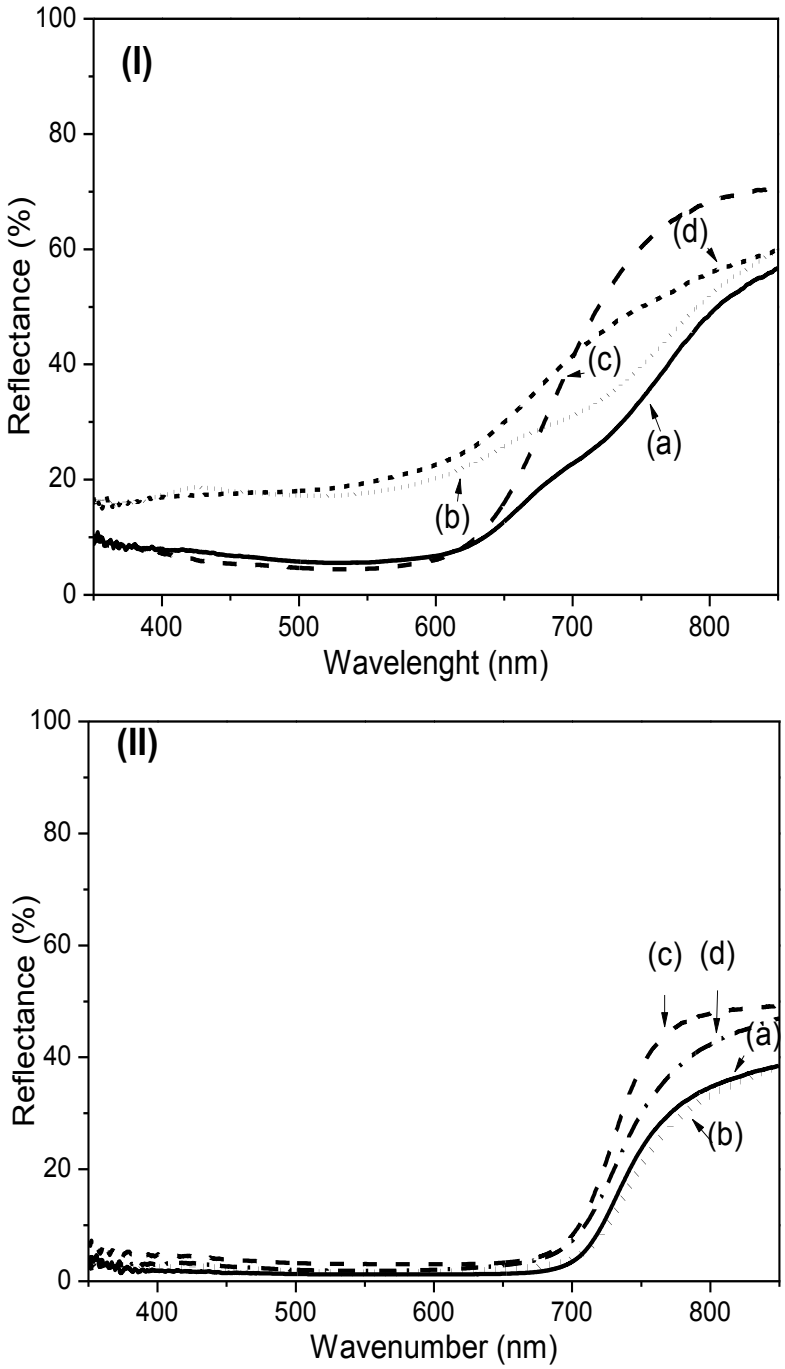

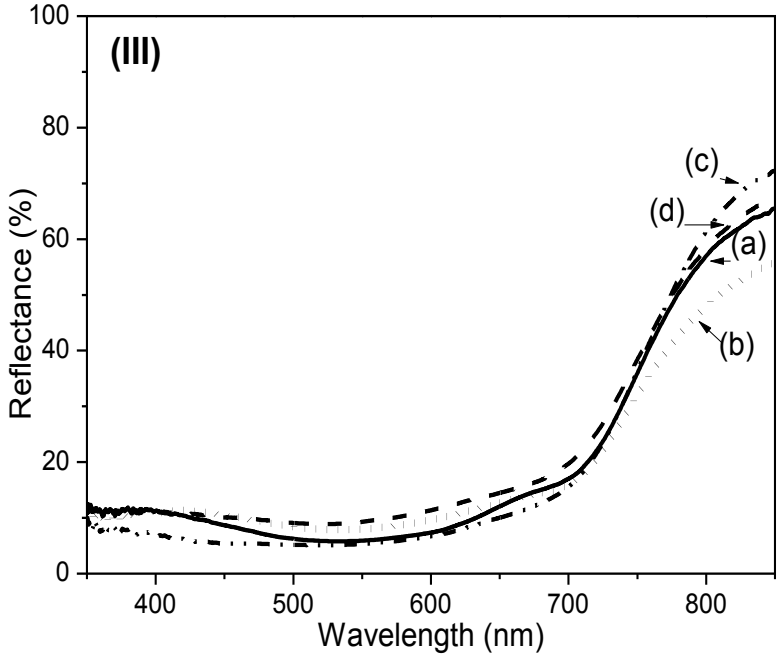

Fig. 8. UV-Vis DR spectra of pigments before and after light exposure for (I) (a) Hec-ALZ at pH 12 before, (b) Hec-ALZ et pH 12 after 192 h, (c) Hec-ALZ at pH 9 before and (d) Hec-ALZ at pH 9 after 192 h; (II) Hec_CTA-ALZ hybrids: (a) CTA_Hec-ALZ at pH 12 before, (b) CTA_Hec-ALZ at pH 12 after 192 h, (c) CTA_Hec-ALZ at pH 9 before and (d) CTA_Hec-ALZ at pH 9 after 192 h and (III) Hec_PEC-ALZ hybrids: (a) PEC_Hec-ALZ at pH 12 before, (b) PEC_Hec-ALZ at pH 12 after 192 h, (c) PEC_Hec-ALZ at pH 9 before and (d) PEC_Hec-ALZ at pH 9 after 192 h.

To quantify the color change more accurately, the chroma parameter was measured by a spectrophotometer over CIE L*, a* and b* scales [52]. The ΔE variation in time light exposure are shown in Fig. 9, which the smaller color difference reveals the better color stability of the pigment [24], [53]. The maximum values of ΔE observed were 24, 13 and 7 for Hec-ALZ pH9, PEC_Hec-ALZ pH9 and CTA_Hec-ALZ at pH9 respectively, and 18, 10 and 4 for Hec-ALZ pH12, PEC_Hec-ALZ at pH12 and CTA_Hec-ALZ at pH12 respectively. These results suggested high stability for hybrids based on CTA_Hec, this is probably due to the protection of the dye in the interlayer space, making a barrier to the oxygen which promotes the photodegradation. In all cases, the hybrids prepared at pH 12 showed lower values of ΔE than those

prepared at pH 9. Indeed, the total deprotonation of dye molecules promoted better interactions with the host.

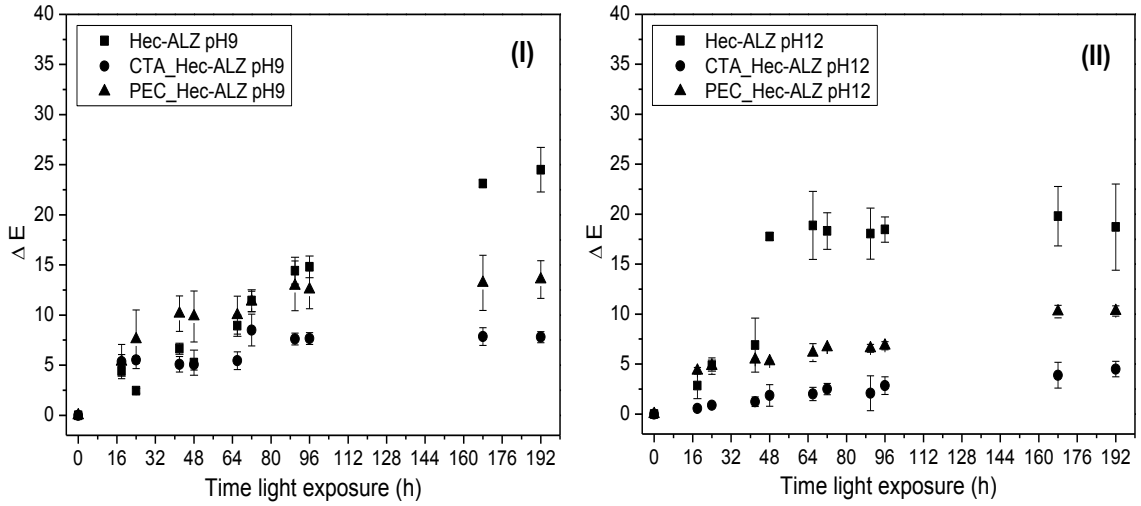

Fig. 9. Color difference (ΔE^*) of (I) pigments obtained at pH 9 and (II) pigments obtained at pH 12 exposed to light for 192 h.

4. Conclusions

Hybrid pigments were prepared by adsorption of ALZ in aqueous solution at pH 9 and 12 on synthetic Hectorite and its organic derivatives. Prepared pigments exhibit different colors associated to the different interactions between each host and guest. Interactions are driven by van der walls forces and/or hydrogen bonds with silanol on the edges of Hectorite or PEC_Hec based pigments. In the case of CTA_Hec-ALZ, electrostatic forces occur. The XRD, FTIR and TG (DTG) results support the intercalation of the surfactant in the hectorite interlayer space (CTA_Hec), the adsorption of pectin on the surface (PEC_Hec), and their interactions with ALZ dye molecule. Oxygen plays a key role in the oxidation process. The protection of the dye into expanded interlayer space of CTA_Hec explain its better stability. For the hybrids based on Hec or PEC_Hec, although the dye molecules are more exposed to oxygen attack due to their adsorption on the surface, the pectin via intermolecular interactions promotes a slight protection of the dye.

Acknowledgments

We acknowledge the financial support from the CAPES/COFEBUB (Project n° 835/15), CAPES and National Council for Scientific and Technological Development (CNPq, Brazil) for financial support (Grant 310921/2017-1, M.G.F, 307460/2016-9, E.C.S.F). The authors thank Sorbonne University and CNRS for funding.

REFERENCES

[1] E. Pecchioni, M. Ricci, O. Vaselli, C. Lofrumento, V. Levchenko, M. Giamello, A. Scala, A. Williams, B. Turchetta, E. Science, V.G. La Pira, Chemical and mineralogical characterization and 14 C dating of white and red pigments in the rock paintings from Nyero (Uganda), Microchem. J. 144 (2019) 329–338. https://doi.org/10.1016/j.microc.2018.09.020.

[2] J. Chazine, Dècouverte de peintures rupestres à Bornéo, Anthropologie. 104 (2000) 459–471.

[3] J. Roset, The prehistoric rock paintings of the Sahara, (1984).

[4] H.E. Ahmed, I.F. Tahoun, I. Elkholy, A.B. Shehata, Y. Ziddan, Identification of natural dyes in rare Coptic textile using HPLC- DAD and mass spectroscopy in museum of Faculty of Arts, Alexandria University, Egypt, Dye. Pigment. 145 (2017) 486–492. https://doi.org/10.1016/j.dyepig.2017.06.035.

[5] B. Szostek, J. Orska-gawrys, I. Surowiec, M. Trojanowicz, I nvestigation of natural dyes occurring in historical Coptic textiles by high-performance liquid chromatography with UV – Vis and mass spectrometric detection, 1012 (2003) 179–192.

[6] A. Doménech-Carbó, M. T. Doménech-Carbó, M. Silva, F. M. Valle-Algarra, J. V. Gimeno-Adelantado, F. Bosch-Reig, R. Mateo-Castro. Screening and mapping of pigments in paintings using scanning electrochemical microscopy (SECM), Analyst 140 (2015) 1065-1075 . https://doi.org/10.1039/c4an01911c.

[7] Kramell, A., Li, X., Csuk, R., M. Wagner, T. Goslar, P.E. Tarasov, N. Kreusel, R. Kluge, C. Wunderlich, Dyes of late Bronze Age textile clothes and accessories from the Yanghai archaeological site , Turfan , China : Determination of the fi bers, color analysis and dating, Quat. Int. 348 (2014) 214–223. https://doi.org/10.1016/j.quaint.2014.05.012.

[8] W. Zeng, Q. Zhou, H. Zhang, X. Qi, One-coat epoxy coating development for the improvement of UV stability by DPP pigments, Dye. Pigment. 151 (2018) 157–164. https://doi.org/10.1016/J.DYEPIG.2017.12.058.

[9] E.Š. Fabjan, Z. Saghi, P.A. Midgley, M. Otoničar, G. Dražić, M. Gaberšček, A.S. Škapin, Diketopyrrolopyrrole pigment core@multi-layer

SiO2 shell with improved photochemical stability, Dye. Pigment. 156 (2018) 108–115. https://doi.org/10.1016/j.dyepig.2018.03.064.

[10] E. Fernández-García, A. Pérez-Gálvez, Carotenoid:β-cyclodextrin stability is independent of pigment structure, Food Chem. 221 (2017) 1317–1321. https://doi.org/10.1016/J.FOODCHEM.2016.11.024.

[11] A. Marzec, J. Rogowski, W. Maniukiewicz, M. Zaborski, M. Kozanecki, Journal of Industrial and Engineering Chemistry Characterization and properties of new color-tunable hybrid pigments based on layered double hydroxides (LDH) and, 70 (2019) 427–438. https://doi.org/10.1016/j.jiec.2018.11.005.

[12] E.M. Moujahid, R. Lahkale, H. Ouassif, F.Z. Bouragba, W. Elhatimi, Dyes and Pigments New organic dye / anionic clay hybrid pigments : Preparation , optical properties and structural stability, Dye. Pigment. 162 (2019) 998–1004. https://doi.org/10.1016/j.dyepig.2018.11.021.

[13] P. Tang, Y. Feng, D. Li, Dyes and Pigments Improved thermal and photostability of an anthraquinone dye by intercalation in a zinc e aluminum layered double hydroxides host, Dye. Pigment. 90 (2011) 253–258. https://doi.org/10.1016/j.dyepig.2011.01.007.

[14] T. Taguchi, Y. Kohno, M. Shibata, Y. Tomita, C. Fukuhara, Journal of Physics and Chemistry of Solids An easy and effective method for the intercalation of hydrophobic natural dye into organo-montmorillonite for improved photostability, J. Phys. Chem. Solids. 116 (2018) 168–173. https://doi.org/10.1016/j.jpcs.2018.01.027.

[15] D. Guillermin, T. Debroise, P. Trigueiro, L. de Viguerie, B. Rigaud, F. Morlet-Savary, S. Balme, J.M. Janot, F. Tielens, L. Michot, J. Lalevee, P. Walter, M. Jaber, New pigments based on carminic acid and smectites: A molecular investigation, Dye. Pigment. 160 (2019) 971–982. https://doi.org/10.1016/j.dyepig.2018.07.021.

[16] G. Zhuang, M. Jaber, F. Rodrigues, B. Rigaud, P. Walter, Z. Zhang, A new durable pigment with hydrophobic surface based on natural nanotubes and indigo: Interactions and stability, J. Colloid Interface Sci. 552 (2019) 204–217. https://doi.org/10.1016/j.jcis.2019.04.072.

[17] L. de Viguerie, M. Jaber, H. Pasco, J. Lalevée, F. Morlet-Savary, G. Ducouret, B. Rigaud, T. Pouget, C. Sanchez, P. Walter, A 19th Century

“Ideal” Oil Paint Medium: A Complex Hybrid Organic–Inorganic Gel, Angew. Chemie - Int. Ed. 56 (2017) 1619–1623. https://doi.org/10.1002/anie.201611136.

[18] G.L.N. Coelho, C.B. Dornelas, K.C.C. Soares, E.P. Dos Santos, A.L. Vergnanini, T.C. Dos Santos, C.R. Rodrigues, H.C. Castro, L.R.S. Dias, L.M. Cabral, Preparation and evaluation of inclusion complexes of commercial sunscreens in cyclodextrins and montmorillonites: Performance and substantivity studies, Drug Dev. Ind. Pharm. 34 (2008) 536–546. https://doi.org/10.1080/03639040701831769.

[19] J. da S. Lopes, W.V. Rodrigues, V.V. Oliveira, A. do N.S. Braga, R.T. da Silva, A.A.C. França, E.C. da Paz, J.A. Osajima, E.C. da Silva Filho, Modification of kaolinite from Pará/Brazil region applied in the anionic dye photocatalytic discoloration, Appl. Clay Sci. 168 (2019) 295–303. https://doi.org/10.1016/j.clay.2018.11.028.

[20] L.N.F. Queiroga, M.B.B. Pereira, L.S. Silva, E.C. Silva Filho, I.M.G. Santos, M.G. Fonseca, T. Georgelin, M. Jaber, Microwave bentonite silylation for dye removal: Influence of the solvent, Appl. Clay Sci. 168 (2019) 478–487. https://doi.org/10.1016/j.clay.2018.11.027.

[21] D.F. Brito, E.C. Da Silva Filho, M.G. Fonseca, M. Jaber, Organophilic bentonites obtained by microwave heating as adsorbents for anionic dyes, J. Environ. Chem. Eng. 6 (2018) 7080–7090. https://doi.org/10.1016/j.jece.2018.11.006.

[22] D. Yue, Y. Jing, J. Ma, C. Xia, X. Yin, Y. Jia, Removal of Neutral Red from aqueous solution by using modified hectorite, Desalination. 267 (2011) 9–15. https://doi.org/10.1016/j.desal.2010.08.038.

[23] G. Zhuang, F. Rodrigues, Z. Zhang, M.G. Fonseca, P. Walter, M. Jaber, Dressing protective clothing: stabilizing alizarin/halloysite hybrid pigment and beyond, Dye. Pigment. 166 (2019) 32–41. https://doi.org/10.1016/j.dyepig.2019.03.006.

[24] H. Chen, Z. Zhang, G. Zhuang, R. Jiang, A new method to prepare ‘Maya red’ pigment from sepiolite and Basic red 46, Appl. Clay Sci. 174 (2019) 38–46. https://doi.org/10.1016/j.clay.2019.03.023.

[25] G.T.M. Silva, C.P. Silva, M.H. Gehlen, J. Oake, C. Bohne, F.H. Quina, Organic/inorganic hybrid pigments from flavylium cations and

palygorskite, Appl. Clay Sci. 162 (2018) 478–486. https://doi.org/10.1016/j.clay.2018.07.002.

[26] P. Trigueiro, F. Rodrigues, B. Rigaud, S. Balme, J.M. Janot, I.M.G. dos Santos, M.G. Fonseca, J. Osajima, P. Walter, M. Jaber, When anthraquinone dyes meet pillared montmorillonite: Stability or fading upon exposure to light?, Dye. Pigment. 159 (2018) 384–394. https://doi.org/10.1016/j.dyepig.2018.06.046.

[27] T. Sánchez, P. Salagre, Y. Cesteros, Ultrasounds and microwave-assisted synthesis of mesoporous hectorites, Microporous Mesoporous Mater. 171 (2013) 24–34. https://doi.org/10.1016/J.MICROMESO.2013.01.001.

[28] P. Trigueiro, S. Pedetti, B. Rigaud, S. Balme, J.M. Janot, I.M.G. dos Santos, R. Gougeon, M.G. Fonseca, T. Georgelin, M. Jaber, Going through the wine fining: Intimate dialogue between organics and clays, Colloids Surfaces B Biointerfaces. 166 (2018) 79–88. https://doi.org/10.1016/j.colsurfb.2018.02.060.

[29] J. Zhang, C.H. Zhou, S. Petit, H. Zhang, S.C. Amsc, S. Key, G.C. Technology, Applied Clay Science Hectorite : Synthesis , modification , assembly and applications, 177 (2019) 114–138. https://doi.org/10.1016/j.clay.2019.05.001.

[30] R.R. Pawar, Lalhmunsiama, P. Gupta, S.Y. Sawant, B. Shahmoradi, S.-M.M. Lee, Porous synthetic hectorite clay-alginate composite beads for effective adsorption of methylene blue dye from aqueous solution, Int. J. Biol. Macromol. 114 (2018) 1315–1324. https://doi.org/10.1016/J.IJBIOMAC.2018.04.008.

[31] J. Ma, S.-Y. Tian, S.-L. Mu, S.-L. Xie, R.-J. Ying, Adsorption Properties of Methylene Blue on ODA-Hectorite: Equilibrium, Kinetic Studies, 104 (2016) 441–446. https://doi.org/10.2991/icmse-16.2016.11.

[32] J. Ma, Y. Jia, Y. Jing, Y. Yao, J. Sun, Kinetics and thermodynamics of methylene blue adsorption by cobalt-hectorite composite, Dye. Pigment. 93 (2012) 1441–1446. https://doi.org/10.1016/j.dyepig.2011.08.010.

[33] C. Xia, Y. Jing, Y. Jia, D. Yue, J. Ma, X. Yin, Adsorption properties of congo red from aqueous solution on modified hectorite: Kinetic and thermodynamic studies, Desalination. 265 (2011) 81–87.

https://doi.org/10.1016/j.desal.2010.07.035.

[34] P. Baskaralingam, M. Pulikesi, V. Ramamurthi, S. Sivanesan, Modified hectorites and adsorption studies of a reactive dye, Appl. Clay Sci. 37 (2007) 207–214. https://doi.org/10.1016/j.clay.2007.01.014.

[35] Y. Shen, X. Yu, Y. Wang, Facile synthesis of modi fi ed rectorite (M-REC) for effective removal of anionic dye from water, J. Mol. Liq. 278 (2019) 12–18. https://doi.org/10.1016/j.molliq.2019.01.045.

[36] M.K.S. Monteiro, V.R.L. de Oliveira, F.K.G. dos Santos, E.L. de Barros Neto, R.H. de Lima Leite, E.M.M. Aroucha, K.N. de Oliveira Silva, Influence of the ionic and nonionic surfactants mixture in the structure and properties of the modified bentonite clay, J. Mol. Liq. 272 (2018) 990–998. https://doi.org/10.1016/j.molliq.2018.10.113.

[37] A. Özcan, Ç. Ömeroğlu, Y. Erdoğan, A.S. Özcan, Modification of bentonite with a cationic surfactant : An adsorption study of textile dye Reactive Blue 19, J. Harzadous Mater. 140 (2007) 173–179. https://doi.org/10.1016/j.jhazmat.2006.06.138.

[38] Z. Veisi, N.D. Gallant, N.A. Alcantar, R.G. Toomey, Colloids and Surfaces B : Biointerfaces Responsive coatings from naturally occurring pectin polysaccharides, 176 (2019) 387–393.

[39] J.P. Maran, V. Sivakumar, K. Thirugnanasambandham, R. Sridhar, Optimization of microwave assisted extraction of pectin from orange peel, Carbohydr. Polym. 97 (2013) 703–709. https://doi.org/10.1016/j.carbpol.2013.05.052.

[40] S.Q. Liew, N.L. Chin, Y.A. Yusof, Extraction and Characterization of Pectin from Passion Fruit Peels, Ital. Oral Surg. 2 (2014) 231–236. https://doi.org/10.1016/j.aaspro.2014.11.033.

[41] V. Tangaraj, J.-M. Janot, M. Jaber, M. Bechelany, S. Balme, Adsorption and photophysical properties of fluorescent dyes over montmorillonite and saponite modified by surfactant, Chemosphere. 184 (2017) 1355–1361. https://doi.org/10.1016/J.CHEMOSPHERE.2017.06.126.

[42] A. Claro, M.J. Melo, S. Schäfer, J.S.S. de Melo, F. Pina, K.J. van den Berg, A. Burnstock, The use of microspectrofluorimetry for the characterization of lake pigments, Talanta. 74 (2008) 922–929. https://doi.org/10.1016/J.TALANTA.2007.07.036.

[43] R.R. Pawar, B.D. Kevadiya, H. Brahmbhatt, H.C. Bajaj, Template free synthesis of mesoporous hectorites: Efficient host for pH responsive drug delivery, Int. J. Pharm. 446 (2013) 145–152. https://doi.org/10.1016/J.IJPHARM.2013.02.021.

[44] I. Vicente, P. Salagre, Y. Cesteros, Preparation of pure hectorite using microwaves, Phys. Procedia. 8 (2010) 88–93. https://doi.org/10.1016/J.PHPRO.2010.10.017.

[45] J. Ma, T. Wang, C. Liu, H. Li, Tunable white-light emission of lanthanide(III) hybrid material based on hectorite, Chinese Chem. Lett. 29 (2018) 321–324. https://doi.org/10.1016/J.CCLET.2017.08.010.

[46] A.F. Cortez Campos, P.H. Michels-Brito, F.G. da Silva, R.C. Gomes, G. Gomide, J. Depeyrot, Removal of direct yellow 12 from water using CTAB-coated core-shell bimagnetic nanoadsorbents, J. Environ. Chem. Eng. (2019) 103031. https://doi.org/10.1016/J.JECE.2019.103031.

[47] D. Cheikh, F. García-Villén, H. Majdoub, M.B. Zayani, C. Viseras, Complex of chitosan pectin and clay as diclofenac carrier, Appl. Clay Sci. 172 (2019) 155–164. https://doi.org/10.1016/j.clay.2019.03.004.

[48] X. Yang, T. Nisar, Y. Hou, X. Gou, L. Sun, Y. Guo, Pomegranate peel pectin can be used as an effective emulsifier, Food Hydrocoll. 85 (2018) 30–38. https://doi.org/10.1016/j.foodhyd.2018.06.042.

[49] E. Pérez, I.A. Ibarra, A. Guzmán, E. Lima, Hybrid pigments resulting from several guest dyes onto γ-alumina host: A spectroscopic analysis, Spectrochim. Acta Part A Mol. Biomol. Spectrosc. 172 (2017) 174–181. https://doi.org/10.1016/J.SAA.2016.04.017.

https://doi.org/10.1016/j.ijbiomac.2018.04.008.

[50] Y. Andriani, K.S. Jack, E.P. Gilbert, G.A. Edwards, T.L. Schiller, E. Strounina, A.F. Osman, D.J. Martin, Organization of mixed dimethyldioctadecylammonium and choline modifiers on the surface of synthetic hectorite, J. Colloid Interface Sci. 409 (2013) 72–79. https://doi.org/10.1016/J.JCIS.2013.07.055.

[51] S. Jo, S.R. Ryu, W. Jang, O.-S. Kwon, B. Rhee, Y.E. Lee, D. Kim, J. Kim, K. Shin, LED illumination-induced fading of traditional Korean pigments, J. Cult. Herit. 37 (2019) 129–136. https://doi.org/10.1016/J.CULHER.2018.11.005.

[52] M. Melville, Soil colour : Its measurement and its designation in models of uniform colour space Soil colour : its measurement and its designation in, (2015) 495–512. https://doi.org/10.1111/j.1365-2389.1985.tb00353.x.

[53] Y.N. Vodyanitskii, A.T. Savichev, The influence of organic matter on soil color using the regression equations of optical parameters in the system CIE-L*a*b*, Ann. Agrar. Sci. 15 (2017) 380–385. https://doi.org/10.1016/J.AASCI.2017.05.023.